AMERICAN SOCIETY FOR MICROBIOLOGY | Infection and Immunity®

HOST RESPONSE AND INFLAMMATION

TRIM32 Drives Pathogenesis in Streptococcal Toxic Shock-Like Syndrome and *Streptococcus suis* Meningitis by Regulating Innate Immune Responses

Xuan OuYang,[a] Jie Guo,[b] Qingyu Lv,[a] Hua Jiang,[a] Yuling Zheng,[a] Peng Liu,[a] Tongyan Zhao,[a] Decong Kong,[a] Huaijie Hao,[b] Yongqiang Jiang[a]

[a]State Key Laboratory of Pathogen and Biosecurity, Institute of Microbiology and Epidemiology, Academy of Military Medical Sciences, Beijing, China
[b]CAS Key Laboratory of Pathogenic Microbiology and Immunology, Institute of Microbiology, Chinese Academy of Sciences, Beijing, China

ABSTRACT *Streptococcus suis* is an emerging zoonotic agent that causes streptococcal toxic shock-like syndrome (STSLS) and meningitis in humans, with high mortality and morbidity. The pathogenesis of both STSLS and central nervous system (CNS) infections caused by *S. suis* is not well understood. TRIM32, a member of the tripartite motif (TRIM) protein family, has been reported to regulate host inflammatory responses. In this study, we showed that TRIM32 deficiency significantly reduced the level of bacteremia and the production of proinflammatory cytokines following severe *S. suis* infection, protecting infected mice from STSLS. The influence of TRIM32 gene deletion on a range of processes known to be involved in *S. suis* meningitis was also examined. Both levels of bacterial loads and indications of brain hemorrhage were reduced in infected *Trim32*$^{-/-}$ mice compared with infected wild-type (WT) controls. We also found that TRIM32 deficiency increased the permeability of the blood-brain barrier (BBB) and the recruitment of inflammatory monocytes during the early course of *S. suis* infection, potentially limiting the development of *S. suis* meningitis. Our results suggest that TRIM32 sensitizes *S. suis*-induced infection via innate immune response regulation.

KEYWORDS *Streptococcus suis*, meningitis, streptococcal toxic shock-like syndrome, TRIM32

Streptococcus suis is an emerging zoonotic pathogen that causes meningitis, endocarditis, arthritis, pneumonia, bacteremia, and sudden death in swine and humans (1). In recent decades, *S. suis* infection has gained increased attention because of evidence that it has been responsible for outbreaks of meningitis in humans in Southeast Asia and of streptococcal toxic shock-like syndrome (STSLS) in two large-scale epidemics in China which had high incidences of mortality (2–4).

Investigations of the Chinese strain of *S. suis* suggest that an early burst of proinflammatory cytokines, known as a cytokine storm, drives the infection's hypervirulence. In particular, epidemiologic data from *S. suis*-infected patients in the Sichuan outbreak indicated that *S. suis* infection caused excessive expression of proinflammatory cytokines, including interferon gamma (IFN-γ), interleukin-1β (IL-1β), tumor necrosis factor alpha (TNF-α), and IL-6, in patients with STSLS during the early phase of the disease (5). Several subsequent experiments using mouse and pig models supported the conclusion that the Chinese epidemic ST7 strain induced an inflammatory cytokine storm (6, 7). Among these proinflammatory cytokines, overproduction of IFN-γ by natural killer cells was found to play a key role in the lethal STSLS associated with the Chinese strain (8). In addition to STSLS, the high mortality of *S. suis* infection is driven by the deadly meningitis that accompanies it. Our previous research suggested that *S. suis* has

Citation OuYang X, Guo J, Lv Q, Jiang H, Zheng Y, Liu P, Zhao T, Kong D, Hao H, Jiang Y. 2020. TRIM32 drives pathogenesis in streptococcal toxic shock-like syndrome and *Streptococcus suis* meningitis by regulating innate immune responses. Infect Immun 88:e00957-19. https://doi.org/10.1128/IAI.00957-19.

Editor Guy H. Palmer, Washington State University

Address correspondence to Huaijie Hao, haohj721@sina.com, or Yongqiang Jiang, jiangyq@bmi.ac.cn.

Received 3 January 2020
Accepted 17 January 2020
Accepted manuscript posted online 27 January 2020
Published 23 March 2020

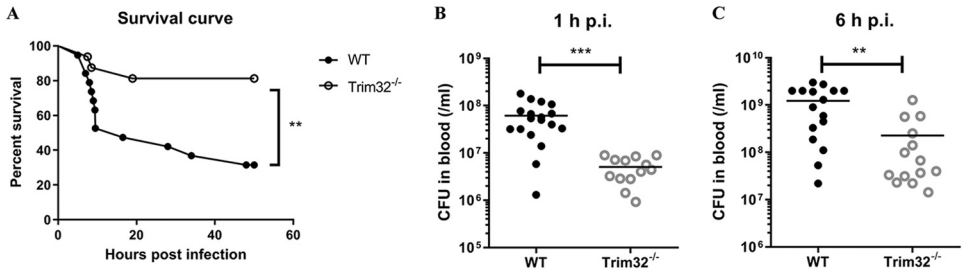

FIG 1 TRIM32 deficiency prevented septic shock resulting from severe *Streptococcus suis* infection. *Trim32*$^{-/-}$ and WT mice were intraperitoneally infected with *S. suis* serotype 2 strain 05ZYH33 (high dose, 2×10^8 CFU). (A) Time-survival curves of *Trim32*$^{-/-}$ and WT mice ($n \geq 16$ each group). The survival rates of the two groups were compared using a log rank test. Each data point indicates an individual mouse. (B and C) The tail vein blood of each mouse was collected at (B) 1 h and (C) 6 h postinfection (p.i.), and colony plate counting was used to determine bacterial loads. WT, wild type. **, $P < 0.01$; ***, $P < 0.001$.

evolved several mechanisms for crossing the blood-brain barrier (BBB) to induce meningitis, including Fhb-Gb3 interaction (9), muramidase-released protein (MRP)-fibrinogen interaction (10), and the remodeling of cytoskeleton mediated by sublytic concentrations of suilysin (11). Once across the BBB, *S. suis* activates TLR2, CD14, and inflammatory cytokines in affected cerebral structures (12). While previous research suggested that *S. suis* induces an unbalanced and damaging immune response, the cellular and molecular mechanisms that trigger this response are poorly understood. The aim of the current study was to investigate the role of a specific protein, TRIM32, in *S. suis*-induced STSLS and meningitis.

TRIM32, a member of the tripartite motif (TRIM) protein family, represents a likely candidate for causing broad and unbalanced cytokine production because of its wide-ranging roles in triggering innate immune responses. TRIM32 has RING finger and B-box and coiled-coil domain structures common to this protein family, along with an additional NHL domain at the C terminus. TRIM32 was initially identified as an HIV-1 tat binding protein and was subsequently demonstrated to target several proteins for ubiquitination, including PIASγ (13), Abl-interactor 2 (14), X-linked inhibitor of apoptosis (XIAP) (15), STING (16), and polymerase basic protein 1 (PB1) of the influenza A virus (17). During immune responses, TRIM32 has complex effects on cytokine production, with previous research demonstrating both that TRIM32 triggers STING-mediated increases in cytokine (specifically IFN-β) production (16) and that TRIM32 deficiency leads to increased serum cytokine levels [specifically those induced by poly(I:C) and lipopolysaccharide (LPS)] and increased death from *Salmonella enterica* serovar Typhimurium infection (18). Given these findings, TRIM32 represents a promising candidate for triggering *S. suis*-induced STSLS and meningitis, but its role in acute bacterial infection and bacterial meningitis remains underexamined.

In the current study, we used *Trim32* knockout (*Trim32*$^{-/-}$) mice in a series of experiments to determine the effect of TRIM32 on the pathogenesis of the Chinese strain of *S. suis* and, in particular, what role it plays in causing the STSLS and meningitis that underpin the infection's high mortality rate. We report for the first time evidence indicating that TRIM32 drives pathogenesis in *S. suis*-induced STSLS and meningitis via its regulatory role in innate immune responses.

RESULTS

TRIM32 deficiency prevented septic shock from severe *Streptococcus suis* infection. The first set of experiments evaluated evidence that TRIM32 triggers immune responses to *S. suis* that lead to STSLS. We first compared the levels of virulence of *S. suis* in *Trim32*$^{-/-}$ and wild-type (WT) mice by measuring bacterial load and mortality. *Trim32*$^{-/-}$ and WT mice were infected intraperitoneally (i.p.) with a high dose (2×10^8 CFU) of *S. suis* strain 05ZYH33. Mortality was monitored for 2 days, and nearly half of the WT mice (9 of 19) were found to have succumbed by 10 h postinfection, whereas only 2 of the 16 *Trim32*$^{-/-}$ mice had succumbed by 10 h postinfection (Fig. 1A). Blood

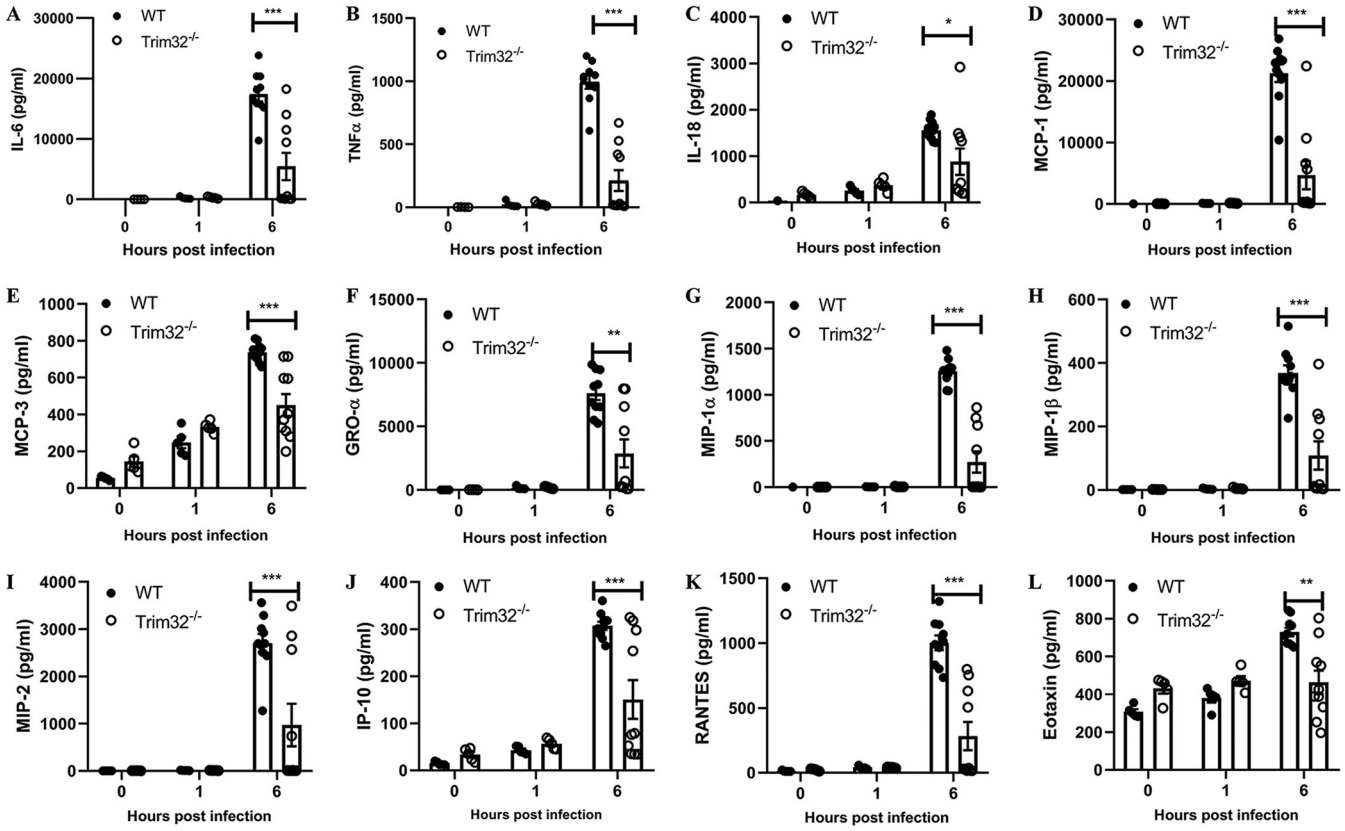

FIG 2 TRIM32 regulates proinflammatory cytokine and chemokine expression upon systemic *S. suis* infection. *Trim32*$^{-/-}$ and WT mice were intraperitoneally infected with *S. suis* serotype 2 strain 05ZYH33 (high dose, 2×10^8 CFU). The levels of proinflammatory (A to C) cytokines and (D to L) chemokines in sera of mice at indicated time points were determined by the use of a Luminex system. WT, wild type. *, $P < 0.05$; **, $P < 0.01$; ***, $P < 0.001$.

bacterial load was determined by colony plate counting at 1 and 6 h postinfection, during the early stages, when we would expect STSLS to manifest in a severe infection. *Trim32*$^{-/-}$ mice had significantly lower blood bacterial loads at both time points than were seen with WT mice (Fig. 1B and C).

Next, we examined evidence that TRIM32 is linked to the cytokine storm which is associated with STSLS and increased mortality. *Trim32*$^{-/-}$ and WT mice were infected i.p. with a high dose (2×10^8 CFU) of *S. suis*, and at 1 and 6 h postinfection, we measured the levels of proinflammatory cytokines, including IL-6, TNF-α, IL-18 (Fig. 2A to C), IL-1β, and those of chemokines, including MCP-1, MCP-3, GROα, MIP-1α, MIP-1β, MIP-2, IP-10, RANTES, and eotaxin (Fig. 2D to L). Compared to WT mice, *Trim32*$^{-/-}$ mice at 6 h postinfection had reduced production of all proinflammatory cytokines and of all chemokines except IL-1β (data not shown).

Because the WT mice had much higher blood bacterial loads as well as higher cytokine levels than the *Trim32*$^{-/-}$ mice, it may be that TRIM32 acts not only by positively regulating the innate immune response but also by increasing systemic dissemination of *S. suis* or inducing higher rates of survival of *S. suis* in the blood, which could then lead to higher cytokine levels. To address this possibility, we employed intravenous (i.v.) injection to infect WT and *Trim32*$^{-/-}$ mice with a high dose (2×10^8 CFU) of *S. suis*. We examined the levels of bacteria in blood at 1 and 6 h postinfection and found no evidence of a difference between WT and *Trim32*$^{-/-}$ mice at 1 h postinfection, while by 6 h postinfection, *Trim32*$^{-/-}$ mice exhibited significant lower levels than WT mice (Fig. 3A). We also determined serum concentrations of cytokines, including TNF-α, IL-18, and IL-6, and of chemokines, including MIP-1α, RANTES, and MCP-1, at 1 h and 6 h postinfection (Fig. 3B). At 1 h postinfection, the WT and *Trim32*$^{-/-}$ mice produced comparable levels of cytokines and chemokines except TNF-α. At 6 h

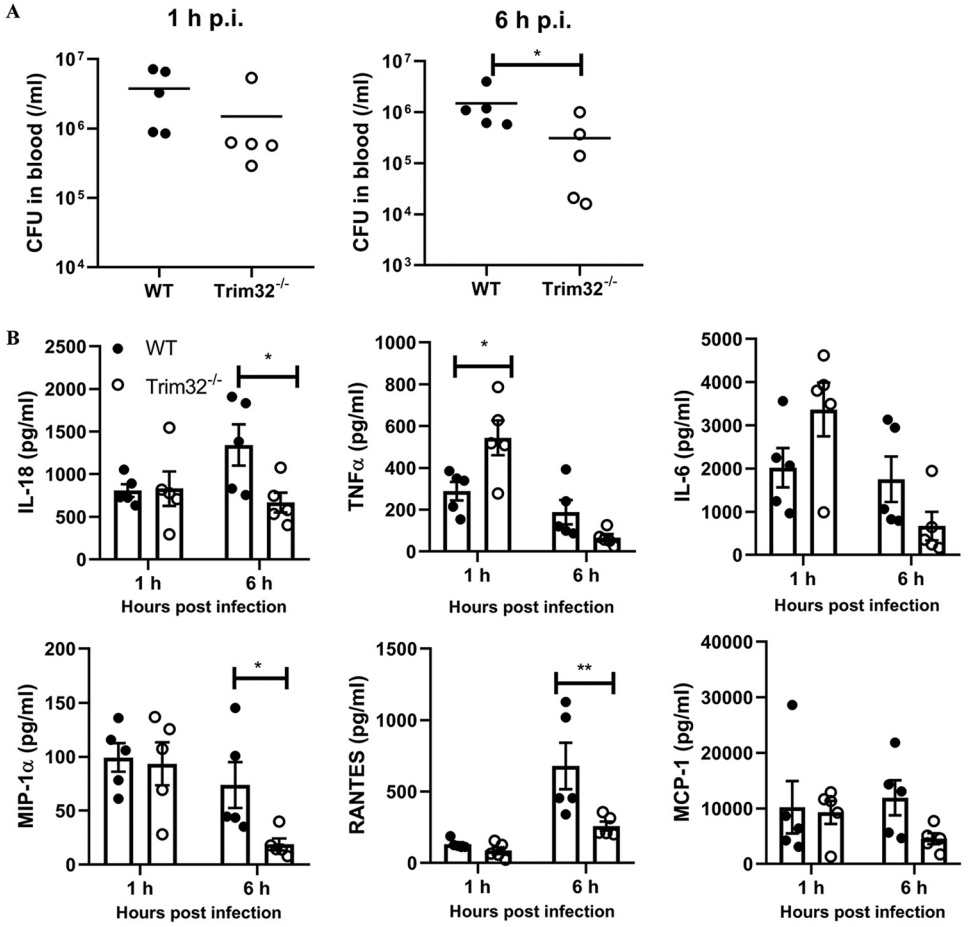

FIG 3 *Trim32*$^{-/-}$ mice exhibited lower levels of bacteremia and cytokines than WT mice. *Trim32*$^{-/-}$ and WT mice were intravenously infected with *S. suis* serotype 2 strain 05ZYH33 (high dose, 2×10^8 CFU). (A) The levels of blood bacteria were determined by colony plate counting at 1 h and 6 h postinfection. (B) The levels of inflammatory cytokines and chemokines in sera from mice 1 h and 6 h postinfection were determined by the use of a Luminex system. WT, wild type. *, $P < 0.05$; **, $P < 0.01$.

postinfection, the *Trim32*$^{-/-}$ mice produced lower levels of all cytokines and chemokines than the WT mice. Moreover, the levels of IL-18, MIP-1α, and RANTES in the serum of WT mice at 6 h postinfection were significantly higher than the levels in serum of *Trim32*$^{-/-}$ mice. In sum, there is some indication that TRIM32 acts to increase systemic dissemination, because bacterial load was higher for WT mice 1 h postinfection following i.p. injection but not i.v. injection. However, our findings also indicate that TRIM32 acts by positively regulating cytokine and chemokine levels, given evidence of higher levels in WT mice 6 h postinfection for both i.p. injection and i.v. injection.

Taken together, these findings indicate that during severe *S. suis* infection, TRIM32 contributes to the survival of *S. suis* in the blood, causing higher levels of bacteremia and triggering an excessive proinflammatory immune response which results in STSLS and higher mortality.

TRIM32 influenced the production of IFN-γ during the early course of infection. While the previous experiments suggested TRIM32 triggers a range of cytokine and chemokine production levels, the next experiments focused on the specific claim that the rapid and lethal STSLS associated with the Chinese strain of *S. suis* is linked to overproduction of IFN-γ, mainly by natural killer cells (8). In order to investigate the role of TRIM32 in IFN-γ production, *Trim32*$^{-/-}$ and WT mice were i.p. infected with a high dose (2×10^8 CFU) of *S. suis* 05ZYH33 to induce toxic shock and with a lower dose (5×10^6 CFU) to enable the development of meningitis. We measured serum levels of

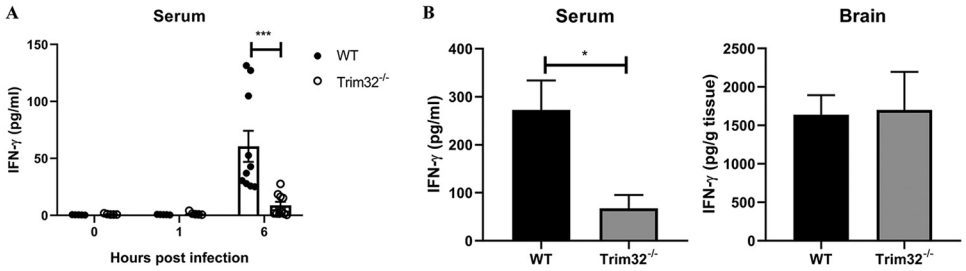

FIG 4 TRIM32 positively regulated the production of IFN-γ in the blood during the early course of *S. suis* infection. (A) *Trim32*$^{-/-}$ and WT mice were intraperitoneally infected with *S. suis* serotype 2 strain 05ZYH33 (high dose, 2×10^8 CFU). Blood samples were harvested at indicated time points, and levels of IFN-γ were measured. (B) *Trim32*$^{-/-}$ and WT mice were intraperitoneally infected with *S. suis* serotype 2 strain 05ZYH33 (lower dose, 5×10^6 CFU). Blood and brain were harvested at 12 h postinfection, and levels of IFN-γ were measured in serum and brain tissue. The levels of IFN-γ in serum and brain were determined by enzyme-linked immunosorbent assay (ELISA). WT, wild type. *, $P < 0.05$; ***, $P < 0.001$.

IFN-γ and found that early in the infection (at 6 h for the high dose or 12 h for the lower dose), both higher (Fig. 4A) and lower (Fig. 4B) doses resulted in more IFN-γ production for WT mice than for *Trim32*$^{-/-}$ mice. Next, we measured brain IFN-γ levels in the mice given the lower dose at 12 h postinfection and found no differences between the mouse phenotypes (Fig. 4B). While the serum measures suggest a role of IFN-γ in the hypervirulence of the Chinese strain of *S. suis*, the lack of an effect on the brain measures is not in keeping with previous research implicating IFN-γ in experimental pneumococcal meningitis and *Streptococcus agalactiae* meningitis (19–21).

TRIM32 deficiency increased resistance to *Streptococcus suis* meningitis. The next set of experiments examined whether TRIM32 plays a role in the pathology of *S. suis*-induced meningitis. *Trim32*$^{-/-}$ and WT mice were i.p. infected with a lower dose (5×10^6 CFU) of *S. suis* 05ZYH33. Bacterial loads were measured in the blood and brain at 5 and 12 h postinfection and in the brain at 2 and 3 days postinfection. Unlike our findings from the early hours of the high-dose infection, the *Trim32*$^{-/-}$ and WT mice had comparable blood bacterial loads at 5 h postinfection (Fig. 5A). However, while the differences did not reach statistical significance, the *Trim32*$^{-/-}$ mice had lower bacterial loads in the blood than the WT mice at 12 h postinfection and in the brain tissue at both 5 h and 12 h postinfection (Fig. 5A and B). In addition, bacterial loads in the brains of *Trim32*$^{-/-}$ mice at day 2 and day 3 postinfection were significantly lower than those of WT mice (Fig. 5C). Finally, we examined the brains of infected mice 3 days postinfection for evidence of hemorrhage, a significant feature of *S. suis* meningitis. The brains of the infected WT mice demonstrated observable brain hemorrhage (Fig. 6A; see also Fig. 7A), which was absent or reduced in level in the infected *Trim32*$^{-/-}$ mice (Fig. 6B). In sum, evidence from the 3-day time course of *S. suis* infection indicates that TRIM32 plays an important role in inducing *S. suis* meningitis.

TRIM32 deficiency increased the permeability of the blood-brain barrier during the early course of *Streptococcus suis* infection. In order to identify the mechanisms by which TRIM32 facilitates meningitis, we evaluated changes in BBB permeability *in vivo*, following i.p. infection with a lower dose (5×10^6 CFU) of *S. suis* 05ZYH33. We administered Evans blue to infected *Trim32*$^{-/-}$ and WT mice at 12 h, 1 day, and 3 days postinfection. Macroscopic inspection of the brain showed more visible penetration of Evans blue in *Trim32*$^{-/-}$ mice than in WT mice at 12 h postinfection (Fig. 7A). Quantitative analysis of extravasated Evans blue confirmed that at 12 h postinfection, the *Trim32*$^{-/-}$ mice had higher levels of Evans blue in the brain lysates than the WT mice. However, there was no significant difference between *Trim32*$^{-/-}$ and WT mice in the levels of extravasated Evans blue at either 1 day or 3 days postinfection (Fig. 7B). These data indicated that TRIM32 deficiency increased the permeability of the BBB during the early course of *S. suis* infection.

TRIM32 deficiency increased the recruitment of PMNs and inflammatory monocytes during the early course of infection. The next set of experiments investigated

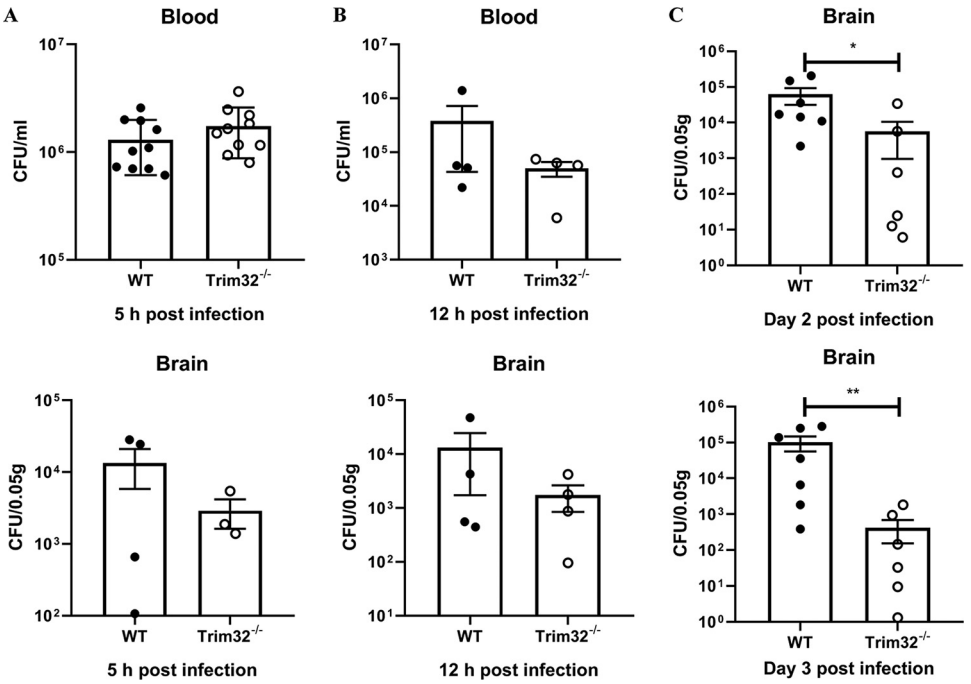

FIG 5 TRIM32 deficiency increased the resistance to *S. suis* meningitis. *Trim32*$^{-/-}$ and WT mice were intraperitoneally infected with *S. suis* serotype 2 strain 05ZYH33 (lower dose, 5×10^6 CFU). Blood and brain samples at (A) 5 h and (B) 12 h postinfection and (C) brain samples at 2 days (top panel) and 3 days (bottom panel) postinfection were taken aseptically, and colony plate counting was used to determine the bacterial loads. WT, wild type.

the possible immune-related outcomes that might occur in response to changes in the BBB by examining immune cell invasion in the brain at 5 h and 12 h postinfection following administration of a lower dose (5×10^6 CFU) of *S. suis*. Flow cytometric analysis was used to identify and measure ranges of immune cell types entering the brain in the early stages of infection. Brain-infiltrating leukocytes were defined as CD45^{high} cells, and a schematic illustrating the gating strategy is given in Fig. 8A, with corresponding results of the flow cytometric analysis given in Fig. 8B. The CD45^{high} population was first divided based on levels of CD11b expression (CD11b$^-$ or CD11b$^+$). The CD11b$^-$ subset was categorized into T cells and B cells based on their expression of CD3 and CD19, respectively. The CD11b$^+$ subset was categorized as corresponding

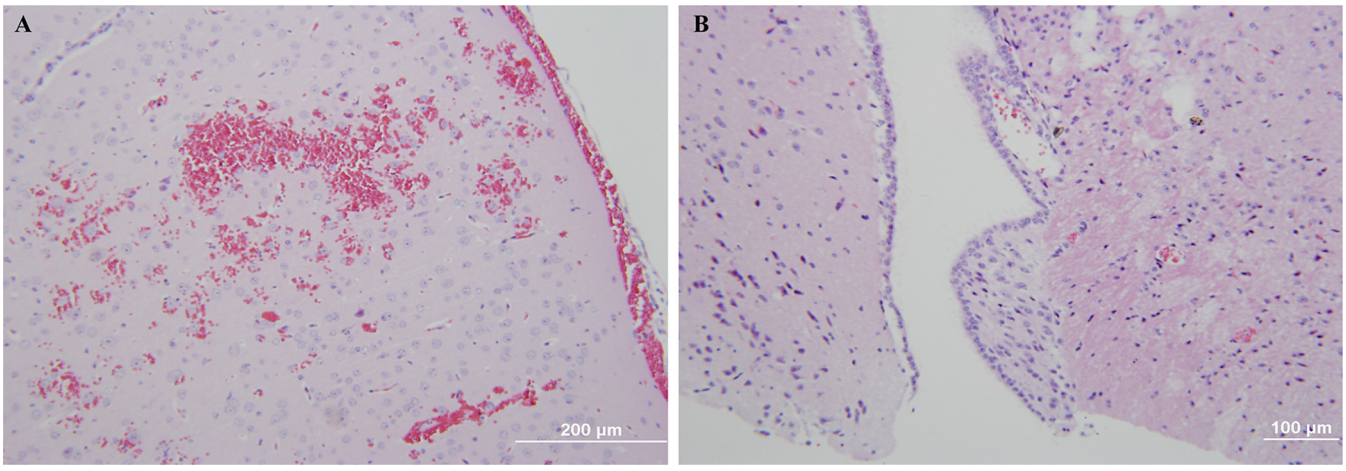

FIG 6 Histopathology of brain tissues from wild-type and Trim32 knockout mice following *S. suis* infection. Hematoxylin and eosin (H&E) staining of infected brain sections from (A) WT and (B) *Trim32*$^{-/-}$ mice at day 3 postinfection with *S. suis* serotype 2 strain 05ZYH33 (lower dose, 5×10^6 CFU) was performed. WT, wild type.

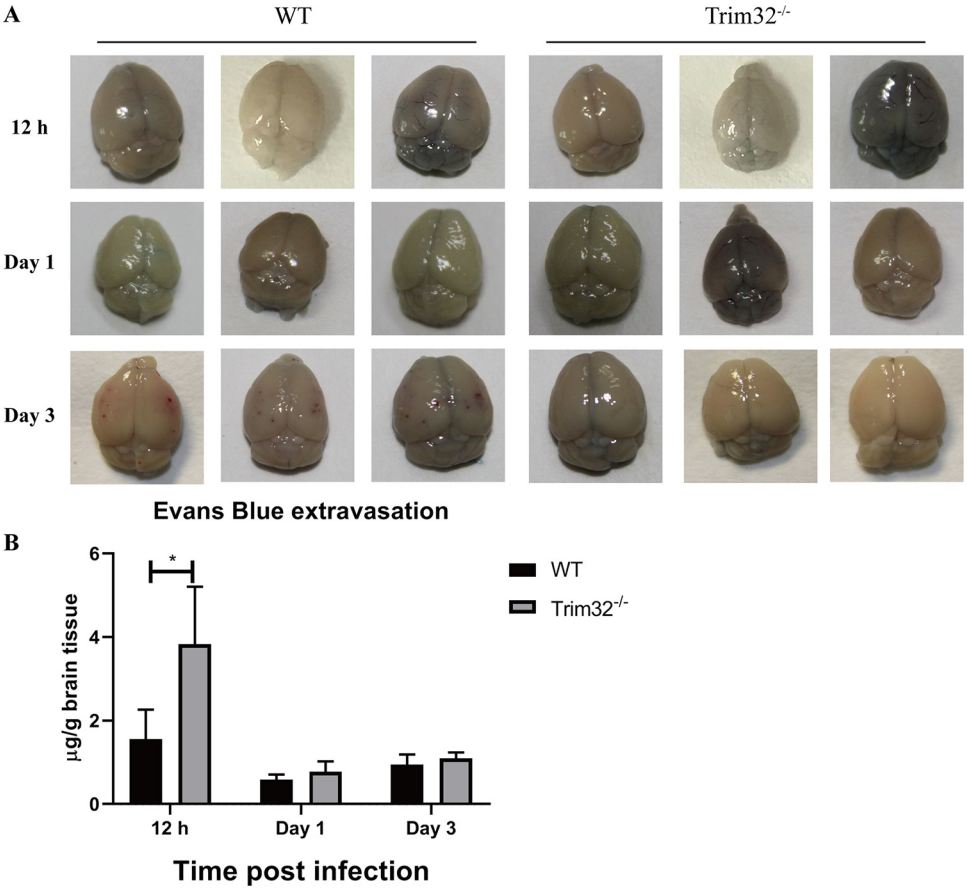

FIG 7 TRIM32 deficiency increased the permeability of the blood-brain barrier during the early course of *S. suis* infection. *Trim32*$^{-/-}$ and WT mice were intraperitoneally infected with *S. suis* serotype 2 strain 05ZYH33 (lower dose, 5×10^6 CFU). (A) Representative images of whole brains stained with Evans blue dyes. (B) Evans blue extravasations in brains. Data are expressed as means ± standard errors of the means (SEM) ($n = 6$ in each group). WT, wild type. *, $P < 0.05$.

to polymorphonuclear neutrophils (PMNs) based on the Ly-6G marker (Ly-6G$^+$). The remaining subset (Ly-6G$^-$) was categorized based on the Ly-6C marker into an inflammatory group (Ly-6C^{high}) and a Ly-6C^{low} group that included monocytes, dendritic cells, and macrophages. For proportional measures, there were no differences at either 5 h or 12 h postinfection between WT and *Trim32*$^{-/-}$ mice in the proportions of brain-invading leukocytes among the total number of live cells or the proportions of PMNs in the invading leukocytes. However, at 12 h postinfection the proportion of inflammatory monocytes among the invading leukocytes was higher in the *Trim32*$^{-/-}$ mice than in the WT mice (Fig. 8C, top row). For counts of cells, the number of brain-invading leukocytes was higher in the *Trim32*$^{-/-}$ mice than in the WT mice at 5 h and 12 h postinfection, the number of PMNs was statistically significantly higher in the *Trim32*$^{-/-}$ than in the WT mice at 5 h postinfection, and the number of inflammatory monocytes was also statistically significantly higher in the *Trim32*$^{-/-}$ than in the WT mice at 12 h postinfection (Fig. 8C, bottom row).

Given the evidence that TRIM32 is linked to higher levels of brain-infiltrating immune cells, we followed up by addressing the possibility that this resulted from differences in levels of immune cells in the blood, rather than from TRIM32-induced recruitment of immune cells into the brain. We used flow cytometry analysis and found that TRIM32 deficiency did not change the proportions (relative to total leukocyte numbers) of major immune cells, including PMNs, monocytes, and T cells, in blood either immediately or at 5 h postinfection (see Fig. S1 in the supplemental material).

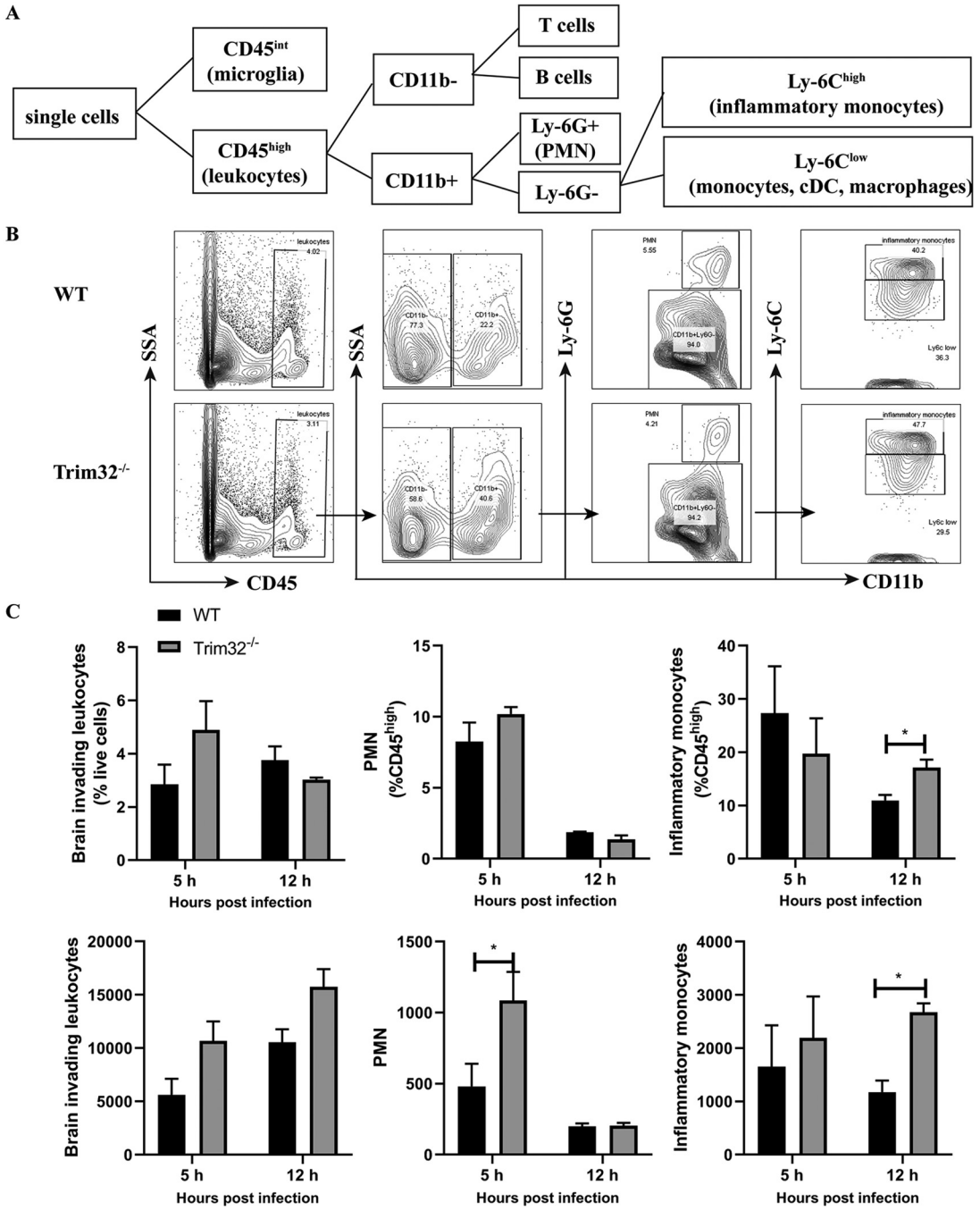

FIG 8 TRIM32 influenced the recruitment of PMNs and inflammatory monocytes to brain during the early course of *S. suis* infection. *Trim32*$^{-/-}$ and WT mice were intraperitoneally infected with *S. suis* serotype 2 strain 05ZYH33 (lower dose, 5×10^6 CFU). Mice were sacrificed at 5 h and 12 h postinfection to analyze early immune cell invasion to the brain. (A) Schematic illustration of the gating strategy. SSA, side scatter. (B) Flow cytometric analysis of leukocytes isolated from a representative mouse brain postinfection. (C) Cell numbers and relative proportions of different invading leukocytes. PMN, polymorphonuclear neutrophils; cDC, classical dendritic cells; WT, wild type. *, $P < 0.05$.

Taken together, these results suggest that TRIM32 deficiency increased the recruitment of PMNs and inflammatory monocytes in the brain during the early course of *S. suis* infection and thus facilitated the clearance of *S. suis* in the brain and eliminated the development of *S. suis* meningitis and subsequent brain injury.

TRIM32 deficiency did not affect the phagocytic and bactericidal ability of macrophages. Our findings thus far support the conclusion that the key impact

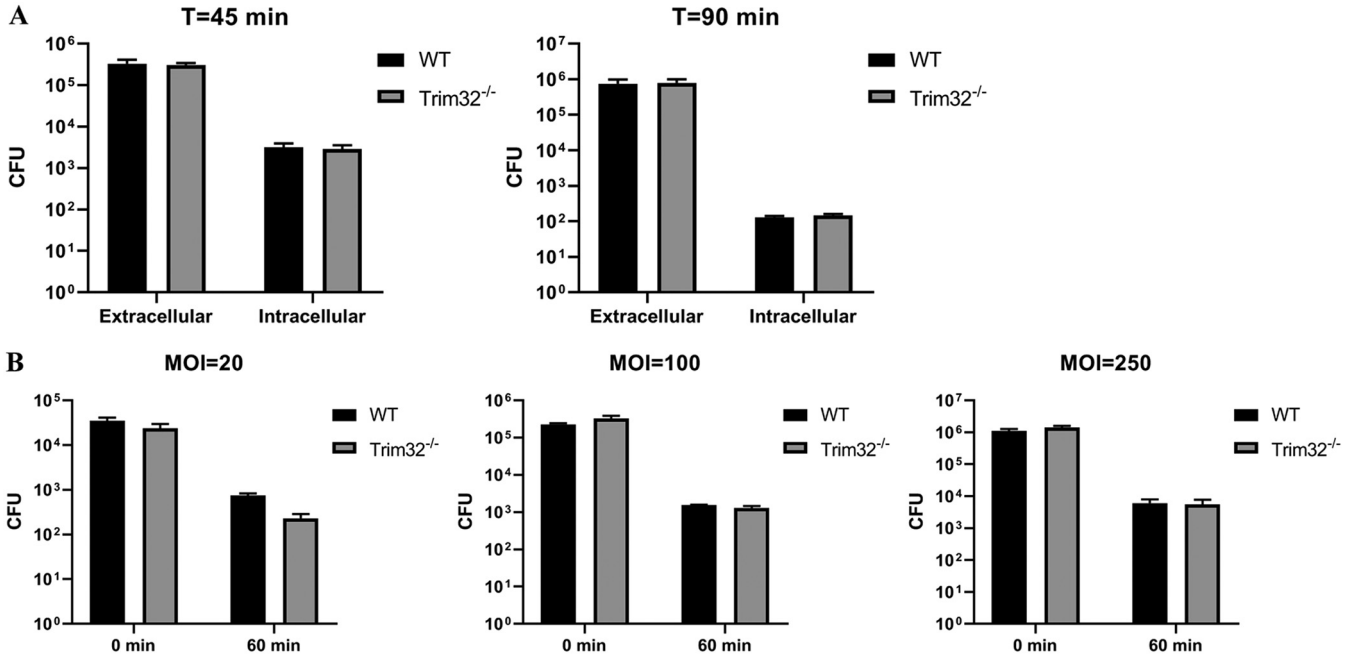

FIG 9 TRIM32 deficiency did not affect the phagocytic and bactericidal ability of macrophages. Peritoneal macrophages (1×10^5 cells) from *Trim32*$^{-/-}$ and WT mice were incubated with *S. suis* serotype 2 strain 05ZYH33 for 15 min to take up the bacteria. (A) Phagocytosis and killing of *S. suis* by macrophages were performed at the MOI of 100. Extracellular and intracellular bacterial levels were evaluated using an antibiotic protection assay after 45 and 90 min of further incubation. (B) Phagocytosis and killing of *S. suis* by macrophages were performed at an MOI of 250, 100, or 20. The numbers of intracellular bacteria were determined by platings after 0 and 60 min of further incubation. WT, wild type.

of TRIM32 is that of increasing the volume of recruited immune cells, and the final set of analyses evaluated the alternative that TRIM32 impairs the effectiveness of immune cells. In particular, we focused on the neutrophils and macrophages which play a key role in clearing bacteria and examined the influence of TRIM32 deficiency on the phagocytic and bactericidal abilities of macrophages. Peritoneal macrophages were infected with *S. suis* strain 05ZYH33 at a multiplicity of infection (MOI) of 100 for 15 min and were then washed twice with medium to remove bacteria not associated with the cells. The phagocytes were further cultured for 45 and 90 min, and we determined the levels of viable intracellular and extracellular bacteria. Our results (Fig. 9A) showed no differences between the WT and *Trim32*$^{-/-}$ macrophages in the CFU numbers of intracellular and extracellular bacteria at 45 or 90 min. We also investigated the influence of different MOIs on the phagocytosis and intracellular killing of macrophages. The experimental results (Fig. 9B) demonstrated that the levels of viable intracellular bacteria from WT cells were comparable to the levels of those from *Trim32*$^{-/-}$ cells infected at the same MOI. These observations indicated that TRIM32 deficiency had no influence on the abilities of macrophages to take up and kill *S. suis*.

DISCUSSION

In this work, we demonstrate the key role of TRIM32 in driving the pathogenesis of STSLS and meningitis induced by the Chinese epidemic strain of *S. suis*. Our results demonstrated that TRIM32 positively regulated the production of proinflammatory cytokines and chemokines following *S. suis* infection, which was subsequently found to be associated with increased bacterial load and reduced survival. We also found that TRIM32 deficiency significantly reduced hemorrhage and bacterial loads in the brain. Finally, we found that TRIM32 deficiency increased the permeability of the BBB and the recruitment of PMNs and inflammatory monocytes during the early course of *S. suis*-induced infection, which may provide the mechanism for the reduced bacterial loads and injury in the brain.

By establishing a link between TRIM32 and cytokine production in *S. suis* infection,

our results help flesh out the hypothesis first put forward in response to the 2005 outbreak of *S. suis*-induced STSLS, i.e., that the hypervirulence of Chinese strain ST7 is due to an excessive proinflammatory response (5). Initial attempts to establish the underpinning mechanisms included genome sequencing, which did not reveal the presence of superantigen or homology genes in the genomes of the Chinese ST7 strain. Comparative genomic analysis indicated that the Chinese ST7 strain evolved from a pathogenic ST1 strain to gain hypervirulence via higher expression of suilysin or other, unknown virulence factors. Clinical investigation of STSLS patients confirmed that the poor disease outcome in *S. suis* infection was due to the triggering of a proinflammatory cytokine cascade (22). Subsequent research implicated IFN-γ production in particular in the rapid and lethal STSLS associated with the Chinese strain (8), and a recent study demonstrated that a high level of NLRP3 inflammasome activation was responsible for the development of the cytokine storm via regulation of mature IL-1β and IL-18 (6). Our results provide another link in the chain of evidence by establishing that TRIM32 is critical for the development of the cytokine storm that precedes STSLS development. Specifically, TRIM32 deficiency reduced production levels of all proinflammatory cytokines and chemokines measured (Fig. 2; see also Fig. 3A) except IL-1β (data not shown) in severe *S. suis* intraperitoneal infection. Our findings are in keeping with previous evidence that TRIM32 positively regulates several innate immune signaling pathways, including the NF-κB signaling pathway (13) and the MAVS-TRIF-MyD88 shared signaling pathway (23). Moreover, it is clear from our findings that the levels of TRIM32-induced cytokine and chemokine production were excessive, because the absence of TRIM32 was associated with better survival.

As with STSLS, our results suggest a clear link between TRIM32 and the development of *S. suis*-induced meningitis. TRIM32 deficiency reduced the hemorrhage and bacterial loads in brain, indicating that TRIM32 sensitized the host to *S. suis* meningitis. Additionally, TRIM32 deficiency increased the permeability of the BBB and the recruitment of inflammatory monocytes into the brain. Given that inflammatory monocytes are involved in the defense against microbial pathogens, our findings suggest that lowered monocyte recruitment in the presence of TRIM32 may allow the development of *S. suis* meningitis.

Although TRIM32 triggers beneficial innate immune responses in a number of contexts, the results from the current study indicate that TRIM32 impairs effective responses during *S. suis* infection. In particular, *Trim32*$^{-/-}$ mice recruited higher levels of PMNs and inflammatory monocytes, which likely account for the associated decrease in bacterial loads, better survival, and reduced brain injury. While further research is needed to unpack the complex effects of TRIM32 seen during *S. suis* infection, our findings are in keeping with previous research demonstrating that TRIM32 both positively and negatively regulates immune responses (16, 18). Additionally, while increased BBB permeability in *Trim32*$^{-/-}$ mice likely accounts for their better bacterial clearance in the brain, the mechanisms underpinning the effect of TRIM32 on the BBB are unclear. A candidate for future research is the role of IFN-γ, whose production was triggered by TRIM32 and which can both positively (24) and negatively (25) affect BBB permeability.

In conclusion, we have demonstrated for the first time the role of TRIM32 in the pathogenesis of *S. suis*-induced STSLS and meningitis and that TRIM32 functions as a trigger for an excessive and damaging innate immune response. Our study results suggest that the effects of TRIM32 should be targeted by future research in developing treatments for *S. suis* infection.

MATERIALS AND METHODS

Bacterial strains and medium and culture conditions. *S. suis* serotype 2 strain 05ZYH33 was used in the present study. This strain was originally isolated from a STSLS patient in China and has been widely used in several experimental models of septic shock and meningitis (9, 22, 26). The bacteria were grown overnight on goat blood agar at 37°C, and isolated colonies were inoculated into THY medium (Todd-Hewitt broth [THB; Difco] plus 0.2% yeast extract), which was incubated overnight at 37°C in a 5% CO_2 atmosphere without agitation. Working cultures were prepared by inoculating 1% dilutions of overnight cultures into new THY medium and culturing for 3 h to mid-log phase (about 3×10^8 CFU/ml) at 37°C in a 5% CO_2 atmosphere without agitation.

Ethics statement. All animals used in this study were housed at the animal center of the Academy of Military Medical Sciences (AMMS), Beijing, China. Animals were cared for in accordance with the principles of laboratory animal care approved in China. All experimental procedures were approved by the Institutional Animal Care and Use Committee of the AMMS.

Generation of Trim32-deficient mice by TALEN. The *Trim32*$^{-/-}$ mice were generated by pronucleus microinjection of transcription activator-like effector nuclease (TALEN) mRNAs, which was conducted at Cygen Biosciences (Guangzhou, China). Briefly, to create a *Trim32*$^{-/-}$ mouse from C57BL/6 mice, exon 2 of the *Trim32* gene (Ensembl accession no. ENSMUSG00000051675) was selected as a TALEN target site. TALEN mRNAs generated by *in vitro* transcription were injected into fertilized eggs to produce knockout mice. The founders were genotyped by PCR followed by DNA sequencing analysis, and the positive-testing founders were bred to the next generation.

Experimental infections of mice with *Streptococcus suis*. In order to examine the mechanisms underpinning *S. suis*-induced STSLS and meningitis in mice, we used the following two dosage levels: a very high dose (2×10^8 CFU) which could induce toxic shock in the early hours of the infection (6) and a lower dose (5×10^6 CFU) which allowed the longer survival rate needed for the development of meningitis at 2 or more days postinfection (9).

In experiments that were focused on the mechanisms of *S. suis*-induced septicemia, wild-type (WT) and *Trim32*$^{-/-}$ mice (6 to 8 weeks old) were inoculated with the higher dose (2×10^8 CFU) of *S. suis* 05ZYH33 in 1 ml of THY medium by intraperitoneal (i.p.) injection or in a 0.2 ml of phosphate-buffered saline (PBS) by intravenous (i.v.) injection. Mortality following i.p. challenge was monitored for 2 days, and at 1 and 6 h following i.p. or i.v. challenge, vein blood from infected mice was collected, serially diluted, and then plated on THB plates to evaluate the bacterial load. Blood was collected at indicated time points and centrifuged at $10{,}000 \times g$ for 5 min to obtain serum. Levels of cytokines and chemokines in the serum were determined using a liquid multiarray system (Luminex) according to the manufacturer's manual.

In experiments that were focused on the mechanisms of *S. suis*-induced meningitis, *Trim32*$^{-/-}$ and WT mice (6 to 8 weeks old) were inoculated with the lower dose (5×10^6 CFU) of *S. suis* 05ZYH33 in 1 ml of THY medium by i.p. injection as previously described (9). The bacterial loads in blood and brain at 5 h, 12 h, 2 days, and 3 days postinfection were determined by colony plate count. To perform histopathological assessment, the brain was removed and fixed with 4% paraformaldehyde. Sections were stained with hematoxylin and eosin and analyzed for brain injury using an Olympus BX53 microscope.

Phagocytosis and killing of *Streptococcus suis*. Phagocytosis and killing of *S. suis* by macrophages were evaluated using an antibiotic protection assay as previously described (27). Murine peritoneal macrophages were prepared using Brewer's thioglycolate medium (28). To determine the phagocytic and intracellular killing ability of peritoneal macrophages, 1×10^5 macrophage cells were cocultivated with *S. suis* for 15 min at 37°C to phagocytize the bacteria. The phagocytes were then washed twice with PRMI medium, and the samples were harvested immediately ($t = 0$) or at the indicated times. To quantify levels of intracellular bacteria, aliquots were treated in parallel with 100 μg gentamicin for 45 min at 4°C to kill the extracellular bacteria. The number of extracellular bacteria was calculated by subtracting the number of intracellular bacteria from the total number of bacteria in the aliquots which had not been treated with gentamicin. The number of CFU in the suspensions was determined by plating each sample on THB agar plates.

Evaluation of blood-brain barrier permeability. The permeability of the BBB was evaluated using Evans blue as previously described (10, 29), with some modifications. Briefly, mice were i.p. injected with 800 μl of 1% (wt/vol) Evans blue dye and perfused transcardially with PBS 1 h later. Extraction of Evans blue dye from the brain was performed to evaluate the BBB leakage (30).

Flow cytometric analysis. In order to examine the infiltration of immune cells into the brain, we used flow cytometry. Mice were euthanized at 5 and 12 h postinfection and perfused transcardially with PBS to remove intravascular blood cells. Brains were then dissected and mechanically dissociated as previously described (31), with some modifications. This involved mashing brains onto nylon screens and digesting the cell suspension with 1 ml collagenase IV (1 mg/ml) and DNase I (200 μg/ml) for 20 min at 37°C with occasional agitation. Following enzymatic digestion, cells were spun down at $286 \times g$ for 5 min at 4°C and resuspended in 5 ml of 25% Percoll–Hanks balanced salt solution (Percoll–HBSS) containing 3% fetal calf serum (FCS) and were then centrifuged at $521 \times g$ for 20 min at room temperature without a break. The upper Percoll layers were carefully removed, the cell pellet was resuspended in HBSS–10% (vol/vol) FCS and centrifuged again at $286 \times g$ for 5 min at 4°C, and the supernatant was then discarded. The cell pellet was resuspended in 1 ml HBSS–10% (vol/vol) FCS.

In order to examine the immune cells in the blood, samples of peripheral blood (~0.3 ml) from WT and *Trim32*$^{-/-}$ mice were collected from tail vein in the presence of EDTA as an anticoagulant. The red blood cells were removed by incubation with ACK (ammonium-chloride-potassium) lysing buffer at room temperature for 3 to 5 min. The white blood cells were collected by centrifugation at $300 \times g$ for 5 min at room temperature and were washed once with phosphate-buffered saline.

Prior to antibody labeling, cell counts and viability were determined by trypan blue exclusion in a hemocytometer. The cell suspension was then incubated with anti-murine CD16/CD32 FC receptor-blocking reagent at 4°C for 10 min to prevent nonspecific binding. The cell suspension was stained with fluorescein isothiocyanate (FITC)-conjugated anti-mouse CD19 (6D5; BioLegend), allophycocyanin (APC)-conjugated anti-mouse CD3 (145-2C11; BD Biosciences), APC-Cy7-conjugated anti-mouse CD45 (30-F11; BioLegend), phycoerythrin (PE)-conjugated anti-mouse Ly6G (RB6-8C5; BioLegend), PE-Cy7-conjugated anti-mouse Ly6C (HK1.4; BioLegend), and peridinin chlorophyll protein (PerCP)-Cy5.5-conjugated anti-mouse CD11b (M1/70; eBioscience). The suspension was then incubated at 4°C for 20 min in the dark.

After staining, the cell suspension was washed with 2 ml of flow cytometric buffer and centrifuged at 350 × *g* at 10°C for 5 min. The supernatant was carefully aspirated, and the cell pellet was resuspended in 500 μl of flow cytometric buffer. All samples were acquired on a BD FACSVerse flow cytometer, and data were analyzed using FlowJo software (TreeStar, Ashland, OR, USA).

Statistical analysis. All data were analyzed using GraphPad Prism software. The Kaplan-Meier method was used to draw survival curves, and a log rank test was used to compare survival rates. Mann-Whitney *U* tests were used to compare groups for bacterial loads in blood and brain samples and for levels of brain-invading leukocytes. In analyses performed with two independent variables, two-way analysis of variance (ANOVA) was used followed by a Sidak's multiple-comparison test. For all tests, a *P* value of <0.05 was considered significant.

SUPPLEMENTAL MATERIAL

Supplemental material is available online only.

SUPPLEMENTAL FILE 1, PDF file, 0.1 MB.

ACKNOWLEDGMENTS

This work was supported by the Beijing Natural Science Foundation (grant no. 5172025), the National Key R&D Program of China (2017YFD0500204), the Natural Science Foundation of China (no. 81772144), the Chinese State Key Project Specialized for Infectious Disease (no. 2018ZX10712001-015, 2018ZX10711001-003-001, and 2018ZX10732401-001-008), and the State Key Laboratory of Pathogen and Biosecurity (Academy of Military Medical Science; no. SKLPBS1436 and SKLPBS1816).

We declare that we have no conflict of interest.

REFERENCES

1. Palmieri C, Varaldo PE, Facinelli B. 2011. Streptococcus suis, an emerging drug-resistant animal and human pathogen. Front Microbiol 2:235. https://doi.org/10.3389/fmicb.2011.00235.
2. Gottschalk M, Segura M, Xu J. 2007. Streptococcus suis infections in humans: the Chinese experience and the situation in North America. Anim Health Res Rev 8:29–45. https://doi.org/10.1017/S1466252307001247.
3. Ye C, Bai X, Zhang J, Jing H, Zheng H, Du H, Cui Z, Zhang S, Jin D, Xu Y, Xiong Y, Zhao A, Luo X, Sun Q, Gottschalk M, Xu J. 2008. Spread of Streptococcus suis sequence type 7, China. Emerg Infect Dis 14:787–791. https://doi.org/10.3201/eid1405.070437.
4. Huong VT, Ha N, Huy NT, Horby P, Nghia HD, Thiem VD, Zhu X, Hoa NT, Hien TT, Zamora J, Schultsz C, Wertheim HF, Hirayama K. 2014. Epidemiology, clinical manifestations, and outcomes of Streptococcus suis infection in humans. Emerg Infect Dis 20:1105–1114. https://doi.org/10.3201/eid2007.131594.
5. Ye C, Zheng H, Zhang J, Jing H, Wang L, Xiong Y, Wang W, Zhou Z, Sun Q, Luo X, Du H, Gottschalk M, Xu J. 2009. Clinical, experimental, and genomic differences between intermediately pathogenic, highly pathogenic, and epidemic Streptococcus suis. J Infect Dis 199:97–107. https://doi.org/10.1086/594370.
6. Lin L, Xu L, Lv W, Han L, Xiang Y, Fu L, Jin M, Zhou R, Chen H, Zhang A. 2019. An NLRP3 inflammasome-triggered cytokine storm contributes to Streptococcal toxic shock-like syndrome (STSLS). PLoS Pathog 15:e1007795. https://doi.org/10.1371/journal.ppat.1007795.
7. Liu M, Fang L, Tan C, Long T, Chen H, Xiao S. 2011. Understanding Streptococcus suis serotype 2 infection in pigs through a transcriptional approach. BMC Genomics 12:253. https://doi.org/10.1186/1471-2164-12-253.
8. Lachance C, Gottschalk M, Gerber PP, Lemire P, Xu J, Segura M. 2013. Exacerbated type II interferon response drives hypervirulence and toxic shock by an emergent epidemic strain of Streptococcus suis. Infect Immun 81:1928–1939. https://doi.org/10.1128/IAI.01317-12.
9. Kong D, Chen Z, Wang J, Lv Q, Jiang H, Zheng Y, Xu M, Zhou X, Hao H, Jiang Y. 2017. Interaction of factor H-binding protein of Streptococcus suis with globotriaosylceramide promotes the development of meningitis. Virulence 8:1290–1302. https://doi.org/10.1080/21505594.2017.1317426.
10. Wang J, Kong D, Zhang S, Jiang H, Zheng Y, Zang Y, Hao H, Jiang Y. 2015. Interaction of fibrinogen and muramidase-released protein promotes the development of Streptococcus suis meningitis. Front Microbiol 6:1001. https://doi.org/10.3389/fmicb.2015.01001.
11. Lv Q, Hao H, Bi L, Zheng Y, Zhou X, Jiang Y. 2014. Suilysin remodels the cytoskeletons of human brain microvascular endothelial cells by activating RhoA and Rac1 GTPase. Protein Cell 5:261–264. https://doi.org/10.1007/s13238-014-0037-0.
12. Domínguez-Punaro M, Segura M, Plante M, Lacouture S, Rivest S, Gottschalk M. 2007. Streptococcus suis serotype 2, an important swine and human pathogen, induces strong systemic and cerebral inflammatory responses in a mouse model of infection. J Immunol 179:1842–1854. https://doi.org/10.4049/jimmunol.179.3.1842.
13. Albor A, El-Hizawi S, Horn E, Laederich M, Frosk P, Wrogemann K, Kulesz-Martin M. 2006. The interaction of Piasy with Trim32, an E3-ubiquitin ligase mutated in limb-girdle muscular dystrophy type 2H, promotes Piasy degradation and regulates UVB-induced keratinocyte apoptosis through NFkappaB. J Biol Chem 281:25850–25866. https://doi.org/10.1074/jbc.M601655200.
14. Kano S, Miyajima N, Fukuda S, Hatakeyama S. 2008. Tripartite motif protein 32 facilitates cell growth and migration via degradation of Abl-interactor 2. Cancer Res 68:5572–5580. https://doi.org/10.1158/0008-5472.CAN-07-6231.
15. Ryu Y, Lee Y, Lee K, Hwang C, Maeng J, Kim J, Seo Y, You K, Song B, Kwon K. 2011. TRIM32 protein sensitizes cells to tumor necrosis factor (TNFα)-induced apoptosis via its RING domain-dependent E3 ligase activity against X-linked inhibitor of apoptosis (XIAP). J Biol Chem 286:25729–25738. https://doi.org/10.1074/jbc.M111.241893.
16. Zhang J, Hu M, Wang Y, Shu H. 2012. TRIM32 protein modulates type I interferon induction and cellular antiviral response by targeting MITA/STING protein for K63-linked ubiquitination. J Biol Chem 287:28646–28655. https://doi.org/10.1074/jbc.M112.362608.
17. Fu B, Wang L, Ding H, Schwamborn J, Li S, Dorf M. 2015. TRIM32 senses and restricts influenza A virus by ubiquitination of PB1 polymerase. PLoS Pathog 11:e1004960. https://doi.org/10.1371/journal.ppat.1004960.
18. Yang Q, Liu T, Lin H, Zhang M, Wei J, Luo W, Hu Y, Zhong B, Hu M, Shu H. 2017. TRIM32-TAX1BP1-dependent selective autophagic degradation of TRIF negatively regulates TLR3/4-mediated innate immune responses. PLoS Pathog 13:e1006600. https://doi.org/10.1371/journal.ppat.1006600.
19. Pettini E, Fiorino F, Cuppone A, Iannelli F, Medaglini D, Pozzi G. 2015. Interferon-γ from brain leukocytes enhances meningitis by type 4 Streptococcus pneumoniae. Front Microbiol 6:1340. https://doi.org/10.3389/fmicb.2015.01340.
20. Yau B, Mitchell A, Too L, Ball H, Hunt N. 2016. Interferon-γ-induced nitric oxide synthase-2 contributes to blood/brain barrier dysfunction and acute mortality in experimental Streptococcus pneumoniae meningitis. J Interferon Cytokine Res 36:86–99. https://doi.org/10.1089/jir.2015.0078.
21. Clarke D, Letendre C, Lecours M, Lemire P, Galbas T, Thibodeau J, Segura M. 2016. Group B streptococcus induces a robust IFN-γ response by

CD4(+) T cells in an in vitro and in vivo model. J Immunol Res 2016: 5290604. https://doi.org/10.1155/2016/5290604.
22. Chen C, Tang J, Dong W, Wang C, Feng Y, Wang J, Zheng F, Pan X, Liu D, Li M, Song Y, Zhu X, Sun H, Feng T, Guo Z, Ju A, Ge J, Dong Y, Sun W, Jiang Y, Wang J, Yan J, Yang H, Wang X, Gao GF, Yang R, Wang J, Yu J. 2007. A glimpse of streptococcal toxic shock syndrome from comparative genomics of S. suis 2 Chinese isolates. PLoS One 2:e315. https://doi.org/10.1371/journal.pone.0000315.
23. Versteeg GA, Rajsbaum R, Sánchez-Aparicio MT, Maestre AM, Valdiviezo J, Shi M, Inn K-S, Fernandez-Sesma A, Jung J, García-Sastre A. 2013. The E3-ligase TRIM family of proteins regulates signaling pathways triggered by innate immune pattern-Recognition receptors. Immunity 38: 384–398. https://doi.org/10.1016/j.immuni.2012.11.013.
24. Rahman M, Ghosh C, Hossain M, Linfield D, Rezaee F, Janigro D, Marchi N, van Boxel-Dezaire A. 2018. IFN-γ, IL-17A, or zonulin rapidly increase the permeability of the blood-brain and small intestinal epithelial barriers: relevance for neuro-inflammatory diseases. Biochem Biophys Res Commun 507:274–279. https://doi.org/10.1016/j.bbrc.2018.11.021.
25. Lee E, Chanamara S, Pleasure DE, Soulika A. 2012. IFN-gamma signaling in the central nervous system controls the course of experimental autoimmune encephalomyelitis independently of the localization and composition of inflammatory foci. J Neuroinflammation 9:510. https://doi.org/10.1186/1742-2094-9-7.
26. Bi L, Pian Y, Chen S, Ren Z, Liu P, Lv Q, Zheng Y, Zhang S, Hao H, Yuan Y, Jiang Y. 2015. Toll-like receptor 4 confers inflammatory response to Suilysin. Front Microbiol 6:644. https://doi.org/10.3389/fmicb.2015.00644.
27. Benga L, Fulde M, Neis C, Goethe R, Valentin-Weigand P. 2008. Polysaccharide capsule and suilysin contribute to extracellular survival of Streptococcus suis co-cultivated with primary porcine phagocytes. Vet Microbiol 132:211–219. https://doi.org/10.1016/j.vetmic.2008.05.005.
28. Layoun A, Samba M, Santos MM. 29 April 2015, posting date. Isolation of murine peritoneal macrophages to carry out gene expression analysis upon Toll-like receptors stimulation. J Vis Exp https://doi.org/10.3791/52749:e52749.
29. Wang T, Town T, Alexopoulou L, Anderson JF, Fikrig E, Flavell RA. 2004. Toll-like receptor 3 mediates West Nile virus entry into the brain causing lethal encephalitis. Nat Med 10:1366–1373. https://doi.org/10.1038/nm1140.
30. Zhang M, Mao Y, Ramirez SH, Tuma RF, Chabrashvili T. 2010. Angiotensin II induced cerebral microvascular inflammation and increased blood-brain barrier permeability via oxidative stress. Neuroscience 171: 852–858. https://doi.org/10.1016/j.neuroscience.2010.09.029.
31. Posel C, Moller K, Boltze J, Wagner DC, Weise G. 12 February 2016, posting date. Isolation and flow cytometric analysis of immune cells from the ischemic mouse brain. J Vis Exp https://doi.org/10.3791/53658:53658.